HAL open science

Insights into the dynamics of local flame extinction events in CH4 -H2 turbulent flames

Kuppuraj Rajamanickam, Franck Lefebvre, Carole Gobin, Gilles Godard, Corine Lacour, Bertrand Lecordier, Armelle Cessou, David Honoré

To cite this version:

Kuppuraj Rajamanickam, Franck Lefebvre, Carole Gobin, Gilles Godard, Corine Lacour, et al.. Insights into the dynamics of local flame extinction events in CH4 -H2 turbulent flames. European Combustion Meeting 2021, Apr 2021, Napoli, Italy. hal-03539645

HAL Id: hal-03539645

https://hal.science/hal-03539645v1

Submitted on 21 Jan 2022

HAL is a multi-disciplinary open access archive for the deposit and dissemination of scientific research documents, whether they are published or not. The documents may come from teaching and research institutions in France or abroad, or from public or private research centers.

L'archive ouverte pluridisciplinaire **HAL**, est destinée au dépôt et à la diffusion de documents scientifiques de niveau recherche, publiés ou non, émanant des établissements d'enseignement et de recherche français ou étrangers, des laboratoires publics ou privés.

Insights into the dynamics of local flame extinction events in CH_4 – H_2 turbulent flames

Kuppuraj RAJAMANICKAM[1], Franck LEFEBVRE[1], Carole GOBIN[1], Gilles GODARD[1], Corine LACOUR[1], Bertrand LECORDIER[1], Armelle CESSOU[1], David HONORE [*, 1]

[1] CORIA-UMR 6614, CNRS, 76801 SAINT ETIENNE DU ROUVRAY CEDEX

Abstract

In the present study, we have experimentally investigated the effect of H_2 addition on the burning characteristics of turbulent flames in a lab-scale bluff-body burner. The burner geometry houses a large blockage ratio cylindrical bluff body (with a provision of central fuel injection) which separates the annular air passage. This work is motivated by the phenomenon where the flame exhibits intermittent oscillations and local extinction because of interaction with large-scale vortices in the shear layer. These extinction events are highly sporadic and cause alterations in the reaction zone height. The H_2 addition has been studied in the past and reduction in the extinction events have been reported. However, the insights into the sporadic local flame sheet extinction and subsequent re-ignition process are not completely understood. To examine this further, we have conducted experiments with the increasing levels of a volumetric proportion of hydrogen (α_{H2}) from 0% - 100 % in a CH_4-H_2 mixture, while thermal power and co annular airflow rate are maintained constant. Time-resolved (5 kHz), simultaneous OH - PLIF, and PIV have been employed to provide a quantitative link between the hydrodynamics of surrounding co-flow and local flame extinction events. Globally, it is observed that the number of local flame extinction events along the shear layer is reduced with H_2 addition, in fact, no such events are witnessed beyond $\alpha_{H2} \geq 0.4$. Local extinction phenomenon leads to unsteadiness in the continuous flame sheet height measured from the burner exit, subsequently, autocorrelation function has been implemented to analyze the time delay associated with peak to peak variations. The obtained time delay values clearly delineate the increased tendency of flame sheet re-ignition with an increase in α_{H2}.

1. Introduction

Hydrogen founds to be a promising carrier in the current mission of energy decarbonization. Industries adopt the strategy of using directly hydrogen as fuel or blending it with natural gas in grid. Hence, the fundamental understanding in the burning characteristics of hydrogenated mixtures (e.g. H_2 + CH_4) becomes indispensable. In the turbulent flames, the difference in the mixture composition alters several parameters like flame speed, heat release, flame shape, flame–vortex interaction, local and global extinction, etc. Understanding these processes is extremely important in the configurations like bluff body, swirl stabilized burner, as, in these systems, flow turbulence and chemistry are tightly coupled [1]. In the present study, we have considered the bluff body burner, which enabled us to study the flame–flow turbulence interactions in a canonical fashion.

Bluff body flows are commonly used in energy and propulsion devices to enhance flame stabilization. The presence of bluff body in the flow stream forms boundary layer at the walls and subsequent flow separation at trailing edge results in the formation of the recirculation zone close to the burner exit. The seminal work of Zukoski [2] highlighted that the hot combustion products residing within the recirculation zone act as an ignition source for the incoming fresh reactants in the shear layer. The shear layer formed between the recirculation zone and the free stream flow is highly unsteady and exhibits high hydrodynamic strain. The flame may undergo local extinction in this zone, and then the fresh mixtures can pass through shear layers and initiates re-ignition with the flame kernel present in the recirculation zone. This process aids in re-establishing the flame [3]. Furthermore, it is showed that, the process of extinction and re-ignition governs the spatial distribution of reactive scalars in the downstream region [4]. This might induce local modifications in the flow field like flow laminarization (due to dilation effects), variation in the recirculation zone size, etc. Such modifications in the flow field and reaction zone significantly affect the combustion dynamics. Past studies [5] have provided evidence of enhancement in reaction rates due to the increase of H, OH radicals in the reaction zone with the H_2 addition. Hence, the higher strain resistance characteristics of hydrogenated methane flames respond adversely to the flow-imposed strain in the recirculation region, thereby, alters the reaction zone structure. The direct visualization of flame and subsequent OH – PLIF measurements presented in [6] clearly demonstrates the change in flame structure. The rapid increase in flame surface area is reported as a manifestation of thermal - diffusive instabilities in H_2 enriched flames [7]. Despite numerous works, the quantitative interpretation linking the local extinction, subsequent modifications in the reaction zone with respect to the H_2 addition is limited. The present results obtained from a canonical bluff-body burner using time-resolved optical diagnostic tools will enrich the fundamental understanding in hydrogenated turbulent flames.

[*] Corresponding author: david.honore@coria.fr

2. Experimental setup and conditions

The bluff-body burner utilized in this study along with key topological features of the resultant mean flow field and OH contour is depicted in Figure 1. It consists in a central fuel injection surrounded by a cylindrical bluff-body and the annular air flow. The working fluids are air, methane, and hydrogen respectively. All the fluid flow rates are controlled using thermal mass flowmeters. The fuel flow rates of CH_4 and H_2 are varied with reference to the different volume concentration levels of H_2 (α_{H2}), such that, the thermal output of the burner is maintained constant (Table 1). The annular air flow rate has been kept constant across all the test conditions. The varying aerodynamic parameters are then central fuel jet velocity and Reynolds number and air/fuel momentum ratio MR (Table 1).

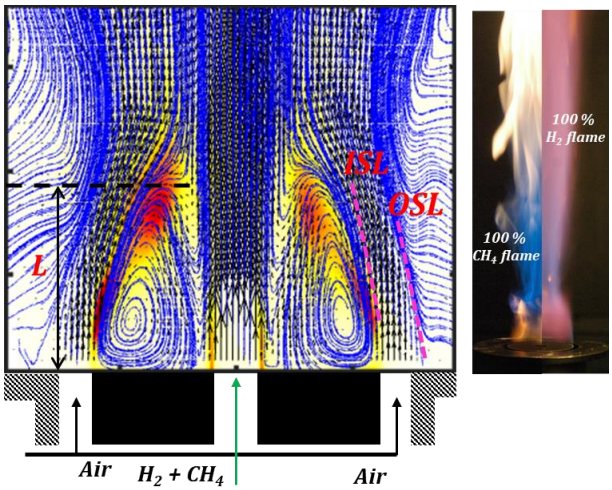

Figure 1 a. Configuration of non-premixed bluff-body burner and flow field with key quantities; b. direct visualization of 100% CH_4 and H_2 flames. ***[OSL, ISL – outer, inner shear layer, L – recirculation zone length]***

Table 1. Experimental conditions

(α_{H2})	Re_{fuel}	Re_{air}	$Power$(kW)	MR
0	4370	10575	16.8	0.25
0.1	4300	10575	16.8	0.26
0.2	4218	10575	16.8	0.28
0.3	4123	10575	16.8	0.31
0.5	3872	10575	16.8	0.38
0.8	3201	10575	16.8	0.42
1	2250	10575	16.8	0.20

2.1 Time-resolved particle imaging velocimetry

The configuration of the time-resolved PIV system is shown in Figure 2. In this study, a double cavity Nd: YAG laser (λ~532 nm; 30 mJ/pulse) with a pulse rate of 10 kHz is used as an illumination source. The laser beam is converted into a thin sheet of ~ 1mm thickness using cylindrical and spherical lenses arrangement. The vertical laser sheet is directed towards the longitudinal axis of the burner. Oxides of zirconium particles are used as a tracing medium (5 µm mean dia.), it should be noted that, both the annulus air and fuel have been seeded separately. The Mie scattering image of seeding particles is recorded using Phantom V2512 camera fitted with Nikon 105 mm lens and 532 nm bandpass filter to avoid the flame emission. The field of view for PIV measurements is chosen as 90 x 90 mm, this yields a spatial resolution of 8.05 pixels/mm. The recorded images are post-processed in Lavision Davis 8.4 software to determine the vector field from an iterative PIV processing with final interrogation windows size of 24 x 24 pixels.

2.2 Time-resolved planar laser-induced fluorescence

Figure 2 illustrates the optics arrangement associated with OH PLIF measurement system. It comprises of Nd: YAG pump laser (λ~532 nm) operating at 10 kHz and tunable dye laser. The dye laser is tuned to produce a laser beam of wavelength ~ 566 nm with the help of Rhodamine 6G dye dissolved with ethanol and further, it is frequency-doubled to emit a UV laser beam of wavelength ~ 283.01 nm; 0.3 mJ/pulse. The generated 283.01 nm beam is used to excite the Q1 (6.5) line of OH radicals in the flame. The UV laser beam is converted to a thin sheet of height ~ 70 mm using sheet-making optics. The UV laser sheet is aligned with the PIV laser sheet to acquire the OH fluorescent image and flow field in the same plane. Since the pulse energy of the UV beam is very low, henceforth, the illumination area for PLIF imaging in the vertical plane is limited to ~ 70 mm. Furthermore, the PLIF laser beam is placed temporally between two PIV laser pulses to enable simultaneous scalar and flow field measurements.

The OH fluorescence image is captured using Photron SA5 camera coupled with a high-speed image intensifier. Nikon UV lens (f4.2, 105 mm) fitted with UG11 and 305 nm bandpass filters are used to capture images at an appropriate wavelength. The above-mentioned filters are especially used to filter out the Mie-scattered signal. OH PLIF images are corrected for the laser sheet height inhomogeneity. Across all the test conditions, images are recorded at 5 kHz with an acquisition time of 2 secs. (i.e. 10000 images per test case).

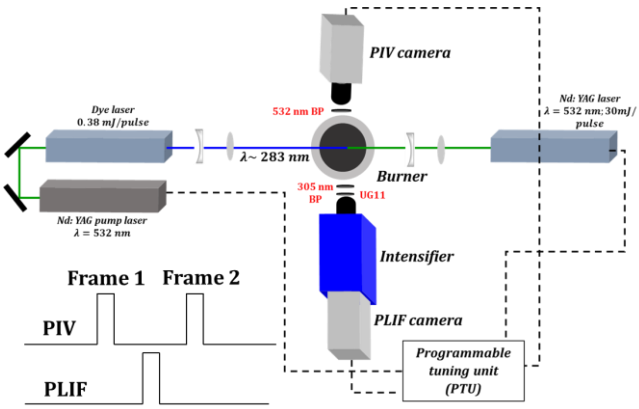

Figure 2 Scheme of the optical setup

3. Global features

The time-averaged flow field superimposed with mean OH contours is illustrated in Figure 3 for several hydrogen proportions. Owing to the symmetric nature,

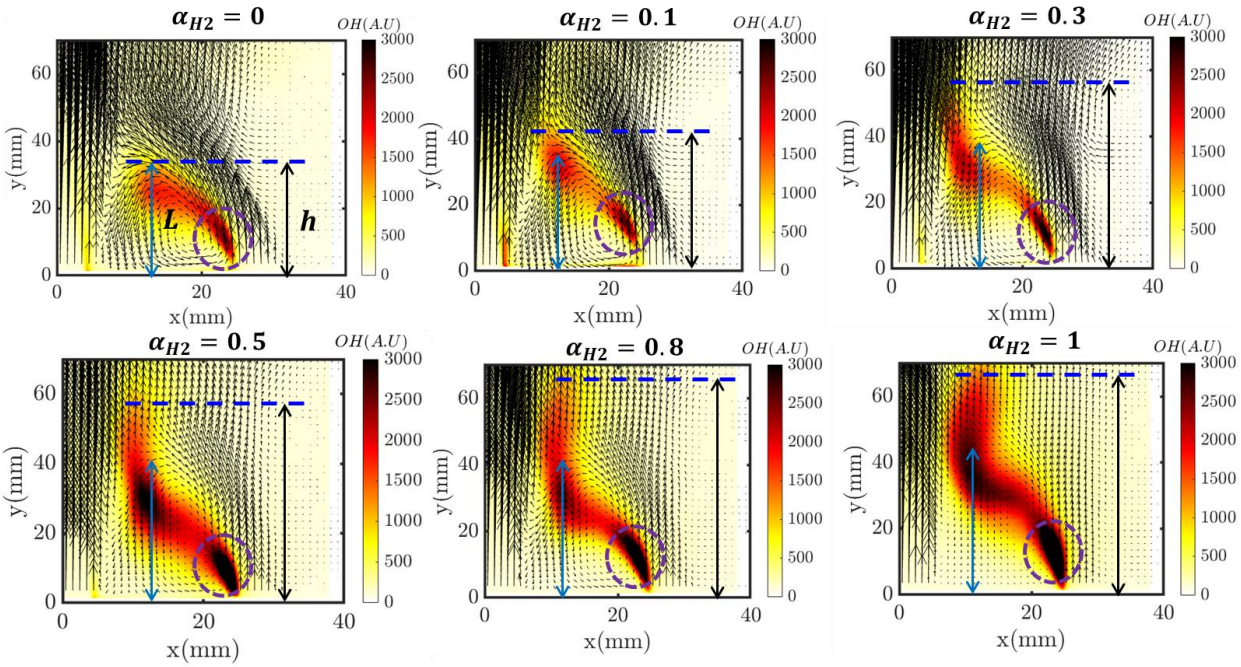

Figure 3 Time-averaged flow field superimposed with mean OH contours

only the right portion of the images are shown here. In a global sense, the flow topology exhibits similar features (relatively) irrespective of H_2 addition. This might be the result of a weak variation in the fuel to annular air jet momentum ratio across all the experimental cases (Table 1). However, variations in the height of the recirculation zone (L) and spatial distribution of OH intensity are observed (h). The stagnation point formed downstream of the recirculation zone (RZ) is used as a marker to locate the recirculation zone height (L). The scale 'h' shown in Figure 3 is just an illustrative representation of the spatial distribution of mean OH contours. The quantitative treatment on reaction zone height derived from the mean of binary images will be presented in the next section. For all the cases, in the RZ, the reaction zone is located in the inner shear layer (ISL) whereas, above the RZ, it is located along with the central fuel jet shear layer. This may be due to the transition in flow topology from recirculating to non-recirculating wake flow, inside and outside RZ respectively.

Besides the variation in 'h', the gradual increase in OH fluorescence intensity is witnessed with H_2 addition, particularly in the ISL region close to the burner exit (shown with purple dotted circles). The increase in OH concentration is known to be a key parameter in promoting reaction rates and thus improved flame stabilization [8]. The detailed experimental and LES results from [9][10] revealed the increase of H radicals in the flame front and subsequent formation of intense OH radicals through chain branching reaction ($H + O_2 \rightarrow O + OH$). Next, the possible reason behind the increase in 'L' can be interpreted from the rise in OH intensity. Authors have shown that, the recirculation zone height is increased with the heating up of the flow [11][12]. The intense heat release (as inferred from OH intensity; Figure 3) and increase in the spatial distribution of flame 'h' with the advent of H_2 addition may induce thermal expansion of the flow due to the rise in the local temperature, which in turn causes the downstream shift of L. Other experiments carried out with constant momentum ratio also depicted the same phenomenon, which clearly suggests a stronger effect of local temperature distribution than the flow aerodynamics. However, unless quantitative temperature measurements it is subtle to describe the mechanism. In the following sections, meticulous efforts have been made to quantitatively understand the governing mechanism behind the spatial distribution of reaction zone.

3.1 Reaction zone intermittency

The unsteadiness associated with the spatial OH distribution in the instantaneous flame contours mandates threshold-based averaging approach to quantitatively represent the reaction zone height [13]. Here, we have employed the algorithm proposed by [14] to obtain the threshold value. Each instantaneous raw OH –PLIF image is converted to a binary image and a total of 10000 images (for each case) are averaged to obtain the flame intermittency distribution. The intermittency value of 0.5 is used as a criterion to mark the reaction zone height (h_f). From Figure 4, it is perceived that, for $0 \sim \alpha_{H2} \leq 0.2$, the value of h_f is ranged from ~ 30 – 40 mm. However, a significant rise in h_f is witnessed beyond $\alpha_{H2} \geq 0.3$ and interestingly it remained at ~ 60 mm from thereon. We shall now look into the governing mechanism behind this process. It is clearly evidenced

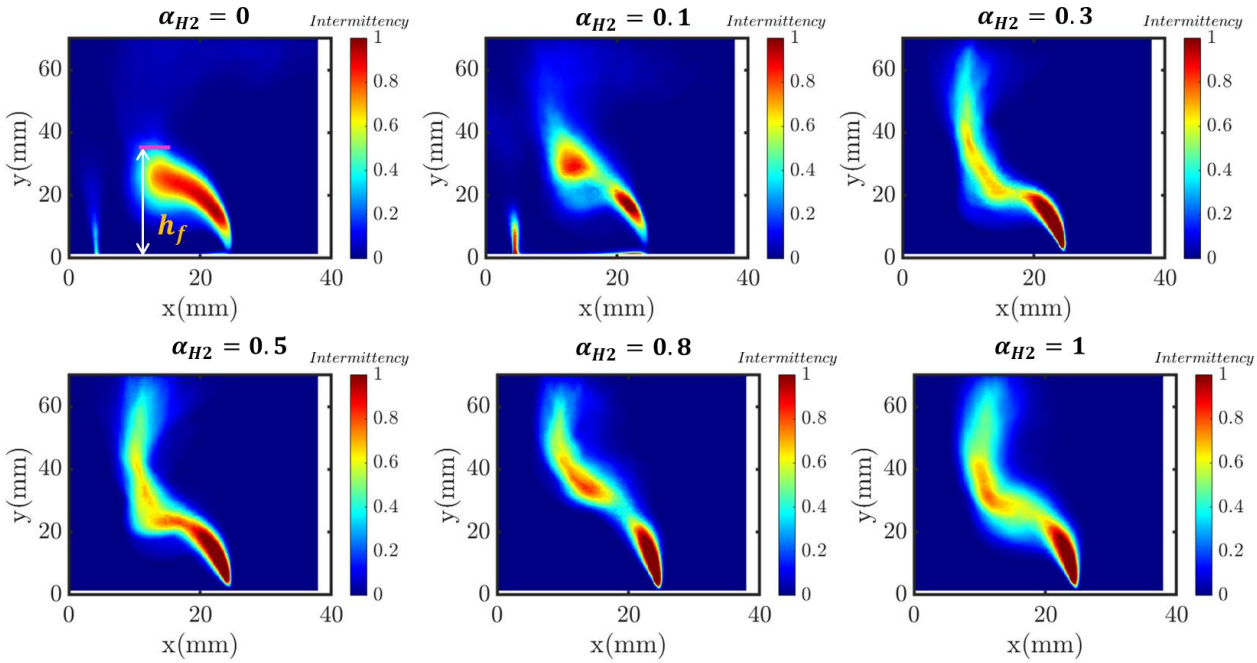

Figure 4 Comparison of the flame intermittency maps

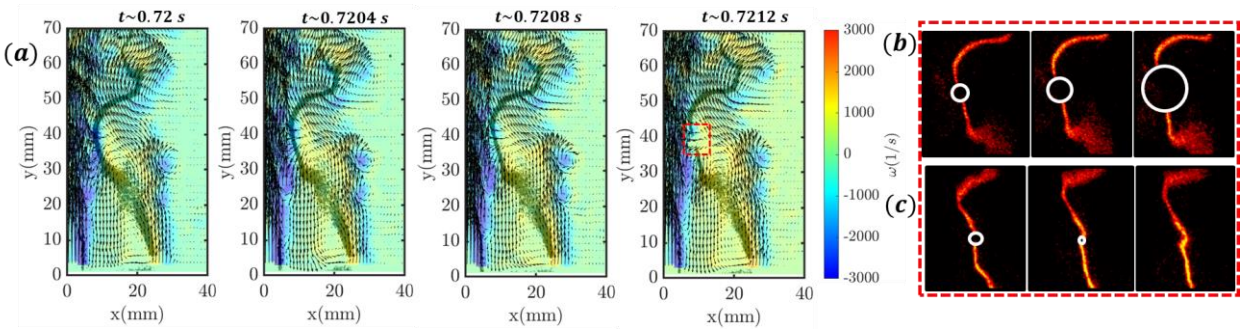

Figure 5 a. Instantaneous visualization of local extinction/hole formation in flame; b, c. sample representation of positive/negative growth of hole size post extinction event.

from the time-averaged images shown in Figure 3, it is perceived that the flame is oriented with an inner shear layer in the spatial domain of $0 < y \leq 40$ mm. The interaction between the turbulent shear layer and wake flow in this region leads to Kelvin Helmholtz (KH-convectively unstable) and Bernard Von Karman instabilities (BVK – absolutely unstable) [15]. The later leads to the formation of large-scale vortical structures. In the downstream location of $y{\sim}L$ where the flow undergoes transition to non-recirculating wake, the streamline possesses intermittent converging and diverging features, which eventually resulted in higher local velocity gradient. Flame usually experiences higher hydrodynamic dynamic strain (κ_{hyd}) in this zone and any excess of κ_{hyd} over the flame extinction strain rate (κ_{ext}) results in local extinction/hole formation in the flame. The temporal sequence of one such event is illustrated in Figure 5a. Followed by local hole formation, two major phenomena are observed, namely, positive (Figure 5 b) and negative growth (Figure 5 c) of hole size. The later can be defined as a closure event, which counterbalances the local extinction i.e. reconnection of flame sheet. The differences in the positive and negative growth rate of hole size determine the reaction zone height in the given time window.

4. Quantitative description of reaction zone height intermittency Vs local extinction process

Section 3.1 highlighted the variations in flame intermittency with H_2 addition; we shall now look into the temporal evolution of reaction zone height across different experimental test cases. To do this, an image-processing scheme is implemented using MATLAB to extract the instantaneous reaction zone height. As illustrated in Figure 6, the processing scheme involves two major steps, first, the raw OH PLIF image segmentation is done based on a user-defined threshold. Second, the bounding box is used to represent each detected object from the image segmentation. The height of the first bounding box from the bottom yields the instantaneous reaction zone height (h'). For brevity, only the time trace of right side height h'_R acquired over the short time window is depicted in Figure 7a. Qualitatively, it is perceived that, the time delay between successive peaks is very long for $0 \leq \alpha_{H2} \leq 0.1$. However, it is significantly reduced for $\alpha_{H2} = 0.2$ and $\alpha_{H2} = 0.3$. It is interesting to note that no local extinction events are

witnessed beyond $\alpha_{H2} > 0.3$, hence, it yields constant value of h'_R. It may be due to the increased level of flame extinction strain (κ_{ext}), as H_2 is known to be favoring it through rise in flame speed. It should be noted that, there may be local extinction even for $\alpha_{H2} > 0.3$, in the far downstream region, however, this is not imaged due to the limitation of FOV in OH – PLIF experiments.

As stated earlier, the flame is subjected to excessive strain in the near vicinity of recirculation zone, due to the interaction of flame front with shear layer generated vortices. It's been reported that, decrease in the flame speed exposes the flame sheet to these vortices [15], thereby the flame undergoes excessive strain that subsequently induces local hole formation. This may be the reason behind the higher probability of local extinction events observed with the low H_2 content test cases.

The histogram plot (Figure 7 b, c) has been generated from the values of h'_R, h'_L acquired over the entire experimental time sequence (i.e. 2 seconds) with a bin size of 15 mm. It is clearly evidenced that, pure methane flame ($\alpha_{H2} = 0$) exhibits higher probability (ρ_n) at ~ 35 – 40 mm across h'_R and h'_L. On contrary, the higher probability got shifted to ~ 60 – 70 mm for $\alpha_{H2} = 0.3$, with a progressive shift towards higher h'_R, h'_L values being observed with the intermediate cases. Now, it is worthwhile to quantify the time lag between successive peaks shown in Figure 7a. To do this, autocorrelation function has been implemented over the h'_R, h'_L values. Since the peak values are randomly distributed, the raw values of h'_R, h'_L are converted into telegraphic signal (0,1) before implementing the autocorrelation.

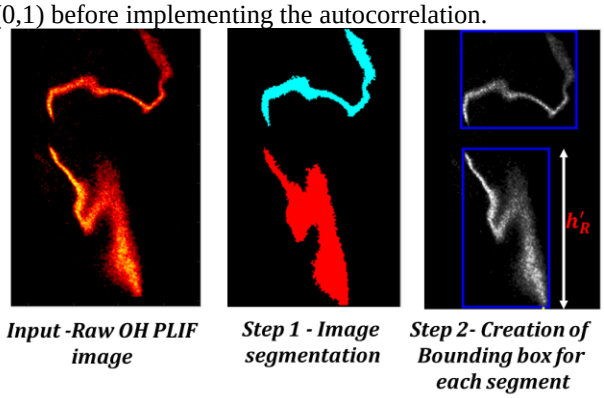

Figure 6. Image processing steps involved in the extraction of instantaneous flame sheet/reaction zone height from OH PLIF images

The crucial step is the identification of cut off value in telegraphic signal conversion. The value at which average of telegraphic signal becomes 0.5 is chosen as a cut off height (Figure 8 a). For instance, ~40 mm and ~62 mm is found be the cut off height for respectively $\alpha_{H2} = 0$ and $\alpha_{H2} = 0.3$ test cases, accordingly, the converted tele signal is illustrated in Figure 8 a. The computed autocorrelation R_{mm} and corresponding time τ lag using equations 1, 2 are presented in Figure 8 b, c, d.

$$R_{mm} = \sum_{i=0}^{N-1} \frac{\left(\{(h')_i - \bar{h}\} - \{(h')_{i+\Delta t} - \bar{h}\}\right)}{\{(h')_i - \bar{h}\}^2} \qquad (1)$$

$$\tau = \lim_{T\to\infty} \frac{1}{T} \int_0^T R_{mm}\, dt \qquad (2)$$

The decay time (τ) founds to be lessening w.r.t α_{H2}. This implies that H_2 addition favors the re-ignition by which flame sheet regains its original height value (i.e. before extinction) in a short duration than non – hydrogenated flame does ($\alpha_{H2} = 0$). The longer time delay associated with $0 \le \alpha_{H2} \le 0.1$, causes a lesser probability for flame presence in the zone beyond the extinction location. It is imperative to say that, this phenomenon limits the reaction zone distribution in the smaller region i.e. $0 < y \le 40$ mm, as evidenced from Figure 4. On the other hand, decrease in the delay time (τ), favors the probability of flame presence and thereby increases the value of h_f. The process of re-ignition in turbulent jet flames can be inferred from the concept of edge flames. Edge flames formed after extinction events govern the re-ignition process [16]. Upon formation, these edge flames either propagate in a forward or backward direction based on the local mixture gradients. The flames with forward propagation is known to initiate the re-ignition and subsequently, the leading, trailing edge formed after the extinction will be attached back to form a stable flame [17]. Authors showed that the flames with higher flame speed (S_L) exhibits the tendency of forward propagation. The study carried out by Ruetsch et.al [18] clearly delineates the increase in S_L with respect to the local heat release due to the reduction in the mixture fraction gradient. In the present study, the increase in heat release with H_2 addition can be corroborated from the OH distribution depicted in Figure 3. Besides, the rise in S_L offers greater resistance to the strain.

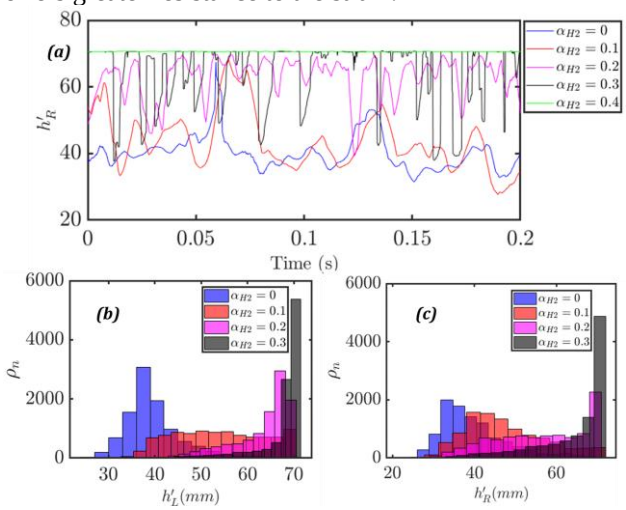

Figure 7 a. Time evolution of instantaneous reaction zone height; b, c – histograms of h'_R, h'_L values

5. Conclusion

The effect of hydrogen addition to methane is experimentally investigated in a canonical bluff-body burner by coupling the time-resolved PIV and OH – PLIF measurements. Globally, the increase in length of the recirculation zone (L) and spatial distribution of reaction zone is noticed with an increase in H_2 content. The thermal expansion induced to the flow due to the local

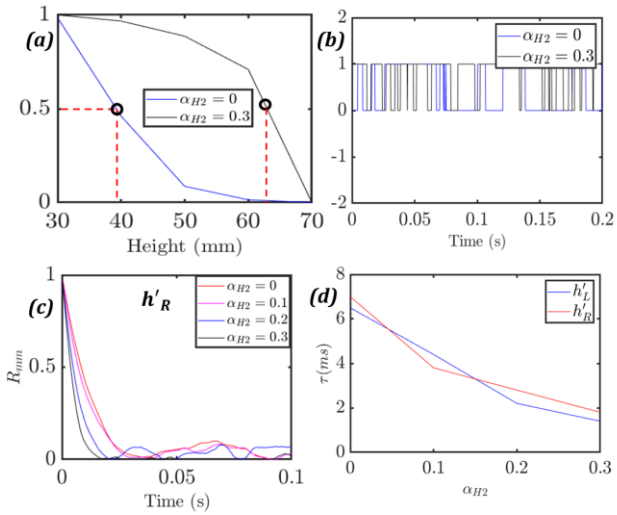

Figure 8 a; steps involved in selection of cut off height; b. Raw height values converted into telegraphic signal; c, – Autocorrelation plot; d – time delay measured from autocorrelation coefficients

rise in the temperature might be the reason behind the former. The quantitative analysis over the physical mechanisms pertains to the latter becomes the main objective of this paper. The instantaneous reaction zone heights extracted from the OH contours show cyclic behavior for the test cases $0 \sim \alpha_{H2} \leq 0.3$. The temporal local extinction encountered in the flames is attributed to the variations in the instantaneous reaction zone height. Subsequently, autocorrelation function is implemented to precisely extract the time delay associated with the intermittent fluctuations. The computed time delay reveals longer value for pure methane, followed by progressive reduction with the hydrogenated flames. This observation quantitatively links the variations encountered in the spatial distribution of the reaction zone with local extinction events. Future work will involve the spatial mapping of species concentration and temperature using spontaneous Raman scattering measurements.

Acknowledgments

This research work is supported by Normandie Regional Council and European Union through European Regional Development Fund (ERDF) in the framework of the RAPHYD project.

6. References

[1] T. W. Davies and J. M. Beer, "Flow in the wake of bluff-body flame stabilizers," in *Symposium (International) on Combustion*, 1971, vol. 13, no. 1, pp. 631–638.

[2] E. E. Zukoski, "Flame stabilization on bluff bodies at low and intermediate Reynolds numbers," PhD Thesis, California Institute of Technology, 1954.

[3] J. P. Longwell, "Flame stabilization by bluff bodies and turbulent flames in ducts," in *Symposium (International) on Combustion*, 1953, vol. 4, no. 1, pp. 90–97.

[4] B. B. Dally, A. R. Masri, R. S. Barlow, and G. J. Fiechtner, "Instantaneous and mean compositional structure of bluff-body stabilized nonpremixed flames," *Combust. Flame*, vol. 114, no. 1–2, pp. 119–148, 1998.

[5] J. L. Gauducheau, B. Denet, and G. Searby, "A numerical study of lean CH4/H2/air premixed flames at high pressure," *Combust. Sci. Technol.*, vol. 137, no. 1–6, pp. 81–99, 1998.

[6] R. W. Schefer, D. M. Wicksall, and A. K. Agrawal, "Combustion of hydrogen-enriched methane in a lean premixed swirl-stabilized burner," *Proc. Combust. Inst.*, vol. 29, no. 1, pp. 843–851, 2002.

[7] E. R. Hawkes and J. H. Chen, "Direct numerical simulation of hydrogen-enriched lean premixed methane–air flames," *Combust. Flame*, vol. 138, no. 3, pp. 242–258, 2004.

[8] H. N. Najm and P. S. Wyckoff, "Premixed flame response to unsteady strain rate and curvature," *Combust. Flame*, vol. 110, no. 1–2, pp. 92–112, 1997.

[9] T. Hussain, M. Talibi, and R. Balachandran, "Investigating the effect of local addition of hydrogen to acoustically excited ethylene and methane flames," *Int. J. Hydrog. Energy*, vol. 44, no. 21, pp. 11168–11184, 2019.

[10] S. Guo, J. Wang, W. Zhang, M. Zhang, and Z. Huang, "Effect of hydrogen enrichment on swirl/bluff-body lean premixed flame stabilization," *Int. J. Hydrog. Energy*, vol. 45, no. 18, pp. 10906–10919, 2020.

[11] M. Namazian, J. Kelly, R. W. Schefer, S. C. Johnston, and M. B. Long, "Nonpremixed bluff-body burner flow and flame imaging study," *Exp. Fluids*, vol. 8, no. 3, pp. 216–228, 1989.

[12] J. A. Lovett, C. Cross, E. Lubarsky, and B. T. Zinn, "A review of mechanisms controlling bluff-body ²stabilized flames with closely-coupled fuel injection," in *Turbo Expo: Power for Land, Sea, and Air*, 2011, vol. 54624, pp. 1275–1287.

[13] E. E. Zukoski, B. M. Cetegen, and T. Kubota, "Visible structure of buoyant diffusion flames," in *Symposium (International) on Combustion*, 1985, vol. 20, no. 1, pp. 361–366.

[14] N. Otsu, "A threshold selection method from gray-level histograms," *IEEE Trans. Syst. Man Cybern.*, vol. 9, no. 1, pp. 62–66, 1979.

[15] T. Lieuwen, S. Shanbhogue, S. Khosla, and C. Smith, "Dynamics of bluff body flames near blowoff," in *45th AIAA Aerospace Sciences Meeting and Exhibit*, 2007, p. 169.

[16] F. Takahashi, W. J. Schmoll, and V. R. Katta, "Attachment mechanisms of diffusion flames," in *Symposium (International) on Combustion*, 1998, vol. 27, no. 1, pp. 675–684.

[17] V. S. Santoro, A. Liñán, and A. Gomez, "Propagation of edge flames in counterflow mixing layers: Experiments and theory," *Proc. Combust. Inst.*, vol. 28, no. 2, pp. 2039–2046, 2000.

[18] G. R. Ruetsch, L. Vervisch, and A. Linán, "Effects of heat release on triple flames," *Phys. Fluids*, vol. 7, no. 6, pp. 1447–1454, 1995.